

Normalizing Flows are Capable Models for RL

Raj Ghugare Benjamin Eysenbach
 Department of Computer Science
 Princeton University
 rg9360@princeton.edu

Abstract

Modern reinforcement learning (RL) algorithms have found success by using powerful probabilistic models, such as transformers, energy-based models, and diffusion/flow-based models. To this end, RL researchers often choose to pay the price of accommodating these models into their algorithms – diffusion models are expressive, but are computationally intensive due to their reliance on solving differential equations, while autoregressive transformer models are scalable but typically require learning discrete representations. Normalizing flows (NFs), by contrast, seem to provide an appealing alternative, as they enable likelihoods and sampling without solving differential equations or autoregressive architectures. However, their potential in RL has received limited attention, partly due to the prevailing belief that normalizing flows lack sufficient expressivity. We show that this is not the case. Building on recent work in NFs, we propose a single NF architecture which integrates seamlessly into RL algorithms, serving as a policy, Q-function, and occupancy measure. Our approach leads to much simpler algorithms, and achieves higher performance in imitation learning, offline, goal conditioned RL and unsupervised RL.¹

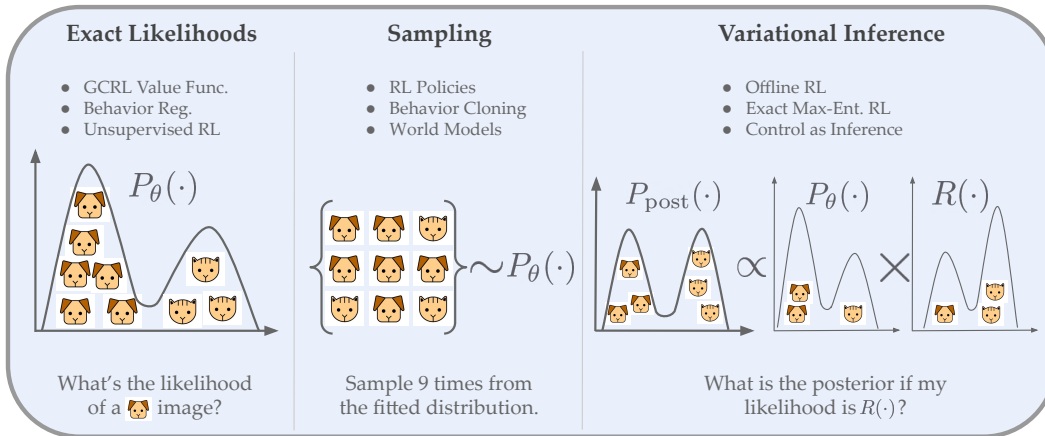


Figure 1: **Probabilistic models and RL.** Three capabilities of probabilistic models important for RL: efficient likelihood computation and sampling, and compatibility with variational inference (VI). These three capabilities are at the core of most RL algorithms and enable myriad applications in RL (See Section 4 for details). For example, behavior cloning requires maximizing likelihoods and sampling [4], GCRL value functions require estimating future discounted state probabilities [22], and MaxEnt RL and RL finetuning requires variational inference [53]. However, models like diffusion / flow matching and autoregressive transformers used in RL today support only a subset of these capabilities, making their application complicated. In this paper, we show how normalizing flow models, which possess these properties, can be a generally capable model family for RL.

¹Project page and code - <https://rajghugare19.github.io/nf4rl/>.

Table 1: **Capabilities of normalizing flows and other probabilistic models.** NFs have capabilities that make them applicable to a large number of algorithms in many RL problems (Section 4), including the ability to compute exact likelihoods, to sample from complex distributions, and to be trained via both maximum likelihood and variational inference (Section 3). Despite these excellent capabilities, research on NFs in RL has been limited compared to other state of the art models. Is this because NFs lack expressivity? Our experiments (Section 6) provide compelling evidence that this is not the case.

Model family	Exact Likelihoods	Sampling	Variational Inference*
Variational Autoencoders	Lower bound	Yes	No
Generative Adversarial networks	No	Yes	No
Energy Based models	Unnormalized	MCMC	No
Diffusion models	Yes, via ODEs	Unrolling SDEs	No
Normalizing Flows	Yes	Yes	Yes

* Although directly performing VI (posterior sampling and estimation) is generally intractable for the first four model families we have still marked them with yellow because additional algorithms for VI do exist [8].

1 Introduction

Reinforcement learning (RL) algorithms often require probabilistic modeling of high dimensional and complex distributions. For example, offline RL or behavior cloning (BC) from large scale robotics datasets requires learning a multi-modal policy [4, 15, 7] and value function estimation in goal-conditioned RL (GCRL) requires estimating probabilities over future goals [22]. Different algorithms require different capabilities, including likelihood estimation, variational inference (VI) and efficient sampling (see Figure 1). A model trained via BC must maximize action likelihoods during training and support fast action sampling for real-time control. Most offline or finetuning RL algorithms require policy models to be able to backpropagate gradients of the value function through sampled actions. For MaxEnt RL with continuous actions, models should be optimizable using variational inference. However, obtaining these abilities in current models often comes at the cost of compute and complexity (Table 1). For example, diffusion models [76] are highly expressive yet computationally demanding: training, sampling, and evaluating log likelihoods all require solving a differential equation. Autoregressive transformer models [84] are scalable and expressive, but are typically limited to discrete settings; using them for RL in continuous spaces requires learning discrete representations of actions [74] or states [59]. Gaussian models offer computational efficiency but lack expressivity. *Can we design expressive probabilistic models which all the capabilities in Fig. 1?*

Normalizing Flows (NFs) are among the most flexible probabilistic models: they (1) support both likelihood maximization and variational inference training, and (2) enable efficient sampling and exact likelihood computation (see Table 1). Yet, NFs have received far less attention from the RL community, perhaps due to the (mis)conception that they have restricted architectures or training instabilities [64]. This paper demonstrates that neither of these notions hold NFs back in practice: NFs can match the expressivity of diffusion and autoregressive models while being significantly simpler. Moreover, unlike other models, NFs do not require additional machinery to be integrated with existing RL frameworks, enabling simpler algorithms that are competitive with if not better than their counterparts.

Our primary contribution is to shed light on the effectiveness and NFs in RL. Building on prior work [45, 19], we develop a simple NF architecture and evaluate it across 82 tasks spanning five different RL settings, including offline imitation learning, offline RL, goal-conditioned RL, and unsupervised RL:

- On offline imitation learning, NFs are competitive with baselines using state of the art generative models such as diffusion and transformers, while using significantly less compute ($6\times$ fewer parameters than diffusion policies).
- On offline conditional imitation learning, NFs outperform BC baselines using models like flow matching, and offline RL algorithms which learn a value function, across 45 tasks.
- On offline RL problems, NFs are competitive with strong baselines using diffusion / flow matching models on most tasks, outperforming all of them on 15/30 tasks.
- On unsupervised GCRL, NFs can rival contrastive learning based algorithms, despite making fewer assumptions.

2 Related Work

Normalizing flows. This work builds on the rich literature of normalizing flow architectures [18, 72, 45, 46, 39, 65, 89]. NICE [18] introduce the idea of stacking neural function blocks that perform shifting, making density estimation efficient. RealNVP [19] extends NICE to non volume preserving layers that also perform a scaling operation. GLOW [45] further propose applying an invertible generalized permutation and a special normalization layer (ActNorm) to improve expressivity.

Probabilistic models in RL. Strides in probabilistic modeling research consistently push the boundaries in deep RL. Variational autoencoders gave rise to a family of model-based [34, 35, 91] and representation learning [51, 88] algorithms. Contrastive learning has been used to learn value functions [58, 73, 24, 61] as well as representations [50, 79] for RL. Advances in sequence modeling led to improvements in BC [13, 10, 52, 74], RL [62, 31] and planning [41]. More recently, diffusion models [78, 37, 76] and their variants [77, 56, 5, 6] have become the popular models for large scale BC pre-training [14, 55, 87, 7], RL finetuning [71, 36], offline RL [2, 67, 85] and planning [40, 90, 57].

NFs in RL. In RL, NFs have been used to learn policies from uncurated data [75] and model exact MaxEnt policies [11, 32, 11]. But despite their flexibility (see Fig. 1 and Table 1), they have not been go-to models in RL; research exploring the application of NFs in RL remains limited. We believe this is because historically, NFs were thought to have limited expressivity [89, 64]. In our experiments, we show that this is not the case (Section 6). We hope that our work brings greater attention towards the potential of NFs in RL, and the development of scalable probabilistic models with similar desirable properties (Fig. 1).

3 Preliminaries

This section describes two major approaches for training probabilistic models and how NFs can be trained using both of them. In the next section, we show that this flexibility allows NFs to be directly plugged into various RL algorithms, improving their expressivity and performance.

Maximum likelihood estimation (MLE). Let $x \in \mathbb{R}^d$ be a random variable with an unknown density $p(x)$. Given a dataset of samples from this density $\mathcal{D} = \{x_i\}_{i=1}^N \sim p(x)$, the goal of MLE is to estimate the parameters of a probabilistic model $p_\theta(x)$ that maximize the likelihood of the dataset:

$$\theta_{\text{MLE}} = \arg \max_{\theta} \mathbb{E}_{x \sim \mathcal{D}} [\log p_\theta(x)]. \quad (1)$$

If $p_\theta(x)$ belongs to a universal family of distributions, then the MLE estimate $p_{\theta_{\text{MLE}}}(x)$ converges towards the true density, as dataset size N increases [42].

Variational inference (VI). In many problems, instead of samples from the true density $p(x)$, one has access to its unnormalized part $\tilde{p}(x) = p(x) \times Z$. The goal of variational inference is to approximate $p(x)$ using a distribution q from some variational family of distributions \mathcal{Q} :

$$q^*(x) = \arg \min_{q \in \mathcal{Q}} D_{\text{KL}}(q || p) = \arg \max_{q \in \mathcal{Q}} \mathbb{E}_{x \sim q(x)} [\log \tilde{p}(x) - \log q(x)], \quad (2)$$

where Z can be ignored from the last equation. If \mathcal{Q} is universal, the global optima of Eq. 2 will be the true density $q^*(x) = p(x)$. To optimize Eq. 2 using gradient descent, one needs to choose a family \mathcal{Q} , from which it is easy generate samples (the expectation requires sampling from q), evaluate likelihoods (second term), and backpropagate through both these operations. Due to these constraints, one typically has to restrict \mathcal{Q} to be a simpler family [43] (e.g., exponential family), or resort to other inference algorithms [30] that require additional complexity (more hyper-parameters or models).

Normalizing flows (NFs). NFs learn an invertible mapping $f_\theta : \mathbb{R}^d \rightarrow \mathbb{R}^d$, from true density $p(x)$ to the a simple prior density $p_0(x)$. This function is parameterized such that the inverse f_θ^{-1} as well as the determinant of its jacobian matrix ($|\frac{df_\theta(x)}{dx}|$) is easily calculable. The learned density $p_\theta(x)$ can then be estimated using the change of variable formula:

$$p_\theta(x) = p_0(f_\theta(x)) \left| \frac{df_\theta(x)}{dx} \right|. \quad (3)$$

To sample from an NF, one first samples from the prior, and return the inverse function:

$$z \sim p_0(x), \text{ and return } x = f_\theta^{-1}(z). \quad (4)$$

Because Eq. (3) and Eq. (4) are passes through a single neural network, back-propagating gradients through them is straightforward. Hence, the NF can be trained efficiently using both MLE (Eq. (1)) and VI (Eq. (2)) [81, 72]:

$$\theta_{\text{MLE}} = \arg \max_{\theta} \mathbb{E}_{x \sim \mathcal{D}} \left[\log p_0(f_\theta(x)) + \log \left(\left| \frac{df_\theta(x)}{dx} \right| \right) \right]. \quad (5)$$

$$\theta_{\text{VI}} = \arg \max_{\theta} \mathbb{E}_{\substack{z \sim p_0(x) \\ x = f_\theta^{-1}(z)}} \left[\log \tilde{p}(x) - \log p_0(z) + \log \left(\left| \frac{df_\theta^{-1}(x)}{dx} \right| \right) \right]. \quad (6)$$

Equation (5) follows from substituting the change of variable formula in Eq. (1). Equation (6) is derived by the same substitution, followed by noting that $z = f_\theta(f_\theta^{-1}(z))$ and $-\log \left(\left| \frac{df_\theta^{-1}(x)}{dx} \right| \right) = \log \left(\left| \frac{df_\theta(x)}{dx} \right| \right)$. It is standard practice to stack multiple such mappings together $f_\theta = f_\theta^1 \circ f_\theta^1 \circ \dots \circ f_\theta^T$. Each mapping is referred to as a *block* in the entire NF.

4 Many RL Algorithms do MLE and VI.

In this section, we first introduce multiple RL problems settings. We will then show how popular representative algorithms in each setting are instantiations of MLE and VI. This will (1) underscore the importance of flexible models that can be directly optimized using MLE and VI, and (2) motivate our use of NFs as a generally capable family of models for RL. We will then describe our architecture in the next section (Section 5). In all the following problems, we assume an underlying controlled markov process \mathcal{M} , with states $s \in \mathcal{S}$ and actions $a \in \mathcal{A}$. The dynamics are $p(s'|s, a)$, the initial state distribution is $p_0(s_0)$ and H is the episode horizon.

4.1 Offline Imitation Learning (IL)

Given a dataset of state-action trajectories $\mathcal{D} = \{s_0^i, a_0^i, \dots, s_H^i\}_{i=1}^N$ collected by an expert(s), the aim in IL is to match the data generating behavior without any environment interactions.

Behavior Cloning (BC) [4, 69] is an algorithm that models the conditional distribution of actions given states directly using MLE:

$$\arg \max_{\theta} \underbrace{\mathbb{E}_{s_t, a_t \sim \mathcal{D}} \left[\log \pi_\theta(a_t | s_t) \right]}_{\text{MLE}}. \quad (7)$$

Goal Conditioned Behavior Cloning (GCBC) [21, 17, 29] is a simple variant of BC which uses a goal $g \in \mathcal{S}$ as additional conditioning information. It is based on the insight that a trajectory leading to any goal, can be treated as an optimal trajectory to reach that goal. Given a state-action pair, a state sampled from the future $p_{t+}(s_{t+} | s_t, a_t)$ is treated as the goal. Formally, GCBC maximizes the following objective:

$$\arg \max_{\theta} \underbrace{\mathbb{E}_{\substack{s_t, a_t \sim \mathcal{D} \\ g_{t+} \sim p(s_{t+} | s_t, a_t)}} \left[\log \pi_\theta(a_t | s_t, g_{t+}) \right]}_{\text{MLE}}. \quad (8)$$

Following prior work [66, 23], we set the future time $t+$ to be a truncated geometric distribution (from $t+1$ to H).

4.2 Offline RL

Offline RL assumes an MDP \mathcal{M} with a reward function $r(s_t, a_t)$. Given a dataset of trajectories $\mathcal{D} = \{s_0^i, a_0^i, r_0^i, \dots, s_H^i, r_H^i\}_{i=1}^N$, the goal is to find a policy $\pi_\theta(a_t | s_t)$, which maximizes the expected discounted return $\mathbb{E}_{\pi_\theta, p} \left[\sum_{t=0}^H \gamma^t r(s_t, a_t) \right]$ [54, 48].

MaxEnt RL + BC [27, 53, 33]. We write out a minimal objective for an offline actor-critic algorithm [27]:

$$\arg \min_{Q_\phi} \mathbb{E}_{\substack{s_t, a_t, r_t, s_{t+1} \sim D \\ a_{t+1} \sim \pi_\theta(\cdot | s_{t+1})}} \left[\left(Q_\phi(s_t, a_t) - r_t - \gamma Q_{\bar{\phi}}(s_{t+1}, a_{t+1}) \right)^2 \right], \quad (9)$$

$$\arg \max_{\pi_\theta} \underbrace{\mathbb{E}_{s_t \sim D, a_t^\pi \sim \pi_\theta(\cdot | s_t)} [Q_\phi(s_t, a_t^\pi) - \lambda \log \pi_\theta(a_t^\pi | s_t)]}_{\text{VI}} + \underbrace{\alpha \mathbb{E}_{s_t, a_t \sim D} [\log \pi_\theta(a_t | s_t)]}_{\text{MLE}}, \quad (10)$$

where $Q_\phi(s, a)$ is the action-value function and $Q_{\bar{\phi}}(s, a)$ denotes the target network [60], λ and α control the strength of the entropy and behavior regularization respectively. For $\lambda = 0$, this algorithm exactly matches TD3+BC [27]. In all our experiments, we use $\lambda = 0$ for minimality². The policy has to sample actions that have high values while staying close to the (potentially multi-modal) behavior policy. NFs ability to be trained using both MLE and VI allows the use of expressive policies, without *any changes* to the simplest offline RL algorithms.

4.3 Goal conditioned RL (GCRL)

GCRL [44] is a multi-task RL problem where tasks correspond to reaching goal states $g \in \mathcal{S}$ sampled from a test goal distribution $p_{\text{test}}(g)$. We will define the discounted state occupancy distribution as $p_{t+}^\pi(s_{t+} | s, a) = (1 - \gamma) \sum_{t=0}^{\infty} \gamma^t p(s_t = s_{t+} | s_0, a_0 = s, a)$.³

Q-function estimation. Prior work has shown that the Q-function for GCRL is equal to the discounted state occupancy distribution $Q^\pi(s, a, g) = p_{t+}^\pi(s_{t+} | s, a)$ [24]. Hence estimating the Q-function can be framed as a maximum likelihood problem:

$$\arg \max_{\theta} \mathbb{E}_{\substack{s_t, a_t \sim D \\ g_{t+} \sim p_{t+}(s_{t+} | s_t, a_t)}} [\log p_\theta(g_{t+} | s_t, a_t)]. \quad (11)$$

MLE

Unsupervised goal sampling (UGS) [25, 68] algorithms do not assume that the test time goal distribution $p_{\text{test}}(g)$ is known apriori. The main aim of UGS is to maximize exploration by commanding goals that are neither too easy nor too difficult for the current agent. This inclines the agent to explore goals on the edge of its goal coverage. But to recognize which goals are on the edge, one needs an estimate of the goal coverage density $p_{t+}(g)$. Many methods [70, 68, 25] primarily fit a density model and then choose goals that have low density. A natural way of estimating densities is MLE, though some prior works use secondary objectives [63, 80, 25, 70] or non-parametric models [68]:

$$\arg \max_{\theta} \mathbb{E}_{\substack{s_t, a_t \sim D \\ g_{t+} \sim p_{t+}(s_{t+} | s_t, a_t)}} [\log p_\theta(g_{t+})]. \quad (12)$$

MLE

Using an estimate of this density, the canonical UGS algorithm is to sample a large batch of goals from the replay buffer and command the agent to reach the goal with the minimum density under $p_\theta(g_{t+})$ [68].

5 A simple and efficient NF architecture for general RL

This section will introduce the NF architecture we use and Section 6 will show how this architecture fits seamlessly into many RL algorithms (those from Section 4). Many design choices affect model expressivity, the speed of computing the forward ($f_\theta(x)$) and inverse ($f_\theta^{-1}(x)$), and the efficiency of computing the determinant of the Jacobian [64]. Our desiderata is to build a *simple* and *fast* architecture that is *expressive enough* to compete and even surpass the most popular approaches across a range of RL problems. To achieve this, we build each NF block f_θ^t by leveraging two components from prior work: (1) a fully connected ‘‘coupling’’ network [19], and (2) a linear flow [45]. In all of our experiments, the model learns a conditional distribution $p_\theta(x | y)$, so each NF block $f_\theta^t : \mathbb{R}^d \times \mathbb{R}^k \rightarrow \mathbb{R}^d$ takes in $y \in \mathbb{R}^k$ as an additional input.

²This is a special case of variational inference. In bayesian inference this corresponds to approximating a maximum a-posteriori estimate.

³We will work with in infinite horizon case, with $H = \infty$.

Coupling network. We use an expressive and simple transformation proposed in Dinh et al. [18, 19]. Let x_t be the input for the t^{th} block and y be the conditioning information. For the t^{th} block, the coupling network $f_\theta^t = \{a_\theta^t, s_\theta^t : \mathbb{R}^{\lfloor d/2 \rfloor} \times \mathbb{R}^k \rightarrow \mathbb{R}^{\lfloor d/2 \rfloor}\}$ does the following computation:

$$(1) x_1^t, x_2^t = \text{split}(x^t), (2) \tilde{x}_2^t = (x_2^t + a_\theta^t(x_1^t, y)) \times \exp(-s_\theta^t(x_1^t, y)), (3) \tilde{x}^t = \text{concat}(x_1^t, \tilde{x}_2^t).$$

Note that the log-det Jacobian of f_θ^t is $-\text{sum}(s_\theta^t(x_1^t, y))$. Further, given \tilde{x}^t and y , the inverse f_θ^{t-1} can be calculated as easily as the forward map (see Appendix B for details).

Linear flow. We adapt the generalized permutation proposed by Kingma and Dhariwal [45] to one dimensional inputs, to linearly transform the output of the coupling layer \tilde{x}^t . The intuition behind adding this linear flow is that each dimension of \tilde{x}^t can be transformed by other dimensions in an end to end manner:

$$x^{t+1} = (\tilde{x}^t)^T W, \text{ where } W = PL_\theta U_\theta, \text{ and } \log |W| = \text{sum} \log(|\text{diag}(U)|).$$

Here, P is a fixed permutation matrix and L_θ is lower triangular with ones on the diagonal and U_θ is upper triangular. Hence, inverting them incurs similar costs as matrix multiplication [64] and calculating the log-det Jacobian requires only the diagonal elements of U .

Normalization. While previous approaches used special variants of normalization layers ([19], [45]), we find that just using LayerNorm [3] in the coupling network’s weights was sufficient of training deep NFs.

Overall, our architecture can be thought of as RealNVP [19] with generalized permutation, or a linear version of GLOW [45] without ActNorm. We have released a simple code for this architecture both in Jax and PyTorch: [code link](#).

6 Experiments

The main aim of our experiments is to use NFs and question some of the standard assumptions across several RL settings. (1) In IL, methods like diffusion policies [14] are popular because they provide expressivity but at a high computational cost. Our experiments with NFs show that this extra compute might not be necessary (Section 6.1). (2) In conditional IL, prior work argues that learning a value function is necessary for strong performance [49, 12, 28, 1]. Our experiments suggest that a sufficiently expressive policy, such as an NF, can often suffice (Section 6.2). (3) In offline RL, auxiliary techniques are typically used to support expressive policies. We show that NF policies can be directly integrated with existing offline RL algorithms to achieve high performance (Section 6.3). (4) In UGS, we show that a single NF can estimate both the value function and goal density, enabling better exploration compared to baseline that make stronger assumptions.

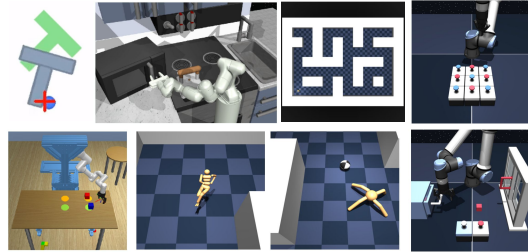


Figure 2: Visualization of tasks

In all experiments, we use the architecture described in Section 5 to implement all algorithms described in Section 4. Implementation details for all algorithms are provided in Appendix A. *Across all problems (IL, offline RL, online GCRL), we present results on a total of 82 tasks (see Fig. 2 for visualization of tasks) with 5 seeds each, which show that NFs are generally capable models that can be effectively applied to a diverse set of RL problems.* Unless stated otherwise, all error bars represent \pm standard deviation across seeds.

6.1 Imitation Learning (IL)

In this section, we use our NF architecture with BC (Section 4.1, Eq. (7)) for imitation learning (NF-BC). Please see implementation details of training and sampling with IL algorithm in Appendix A.1.

Figure 4: BC baselines architectures

Algorithm	Model types
BeT	Transformer.
VQ-BeT	Transformer + VQ-VAEs.
DiffPolicy-C	Convolutional network.
DiffPolicy-T	Transformer.
NF-BC	Fully connected NFs.

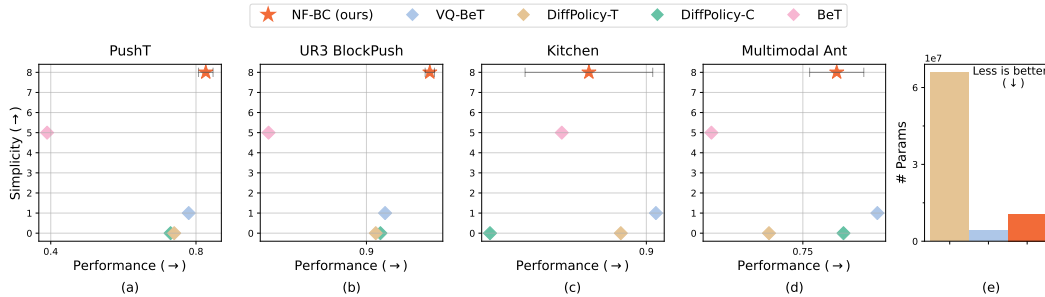


Figure 3: **Imitation Learning.** (a – d) Results on multi-modal behavior datasets which require fine grained control and expressivity. Simplicity is measured by the inverse of the number of hyper-parameters (see Appendix D for details) and performance is measured using normalized rewards. NF-BC is the simplest method, using 2 to 3 times less hyper-parameter than VQ-BeT and DiffPolicy, and performs competitively on all tasks. It outperforms DiffPolicy [14] and VQ-BeT [52] on 2/4 tasks, (e) while using only a fraction of parameters compared to DiffPolicy-C. These results challenge the notion that NFs are inexpressive. We only report standard errors for our methods as baseline results were taken from prior work which did not include error bars [52].

Tasks. PushT requires fine-grain control to maneuver a T-block in a fixed location. Performance is measured by the final normalized area of intersection between the block and the goal. Multimodal Ant, UR3 BlockPush, and Kitchen contain multiple behaviors (4, 2, and 4 respectively). Performance is measured by the normalized number of distinct behaviors the agent is able to imitate successfully over 50 independent trials. We also report the simplicity of algorithms, as it is often a decisive factor in determining whether the algorithm can be practically employed. Simplicity is measured by the negating the number of hyperparameters used. We list and briefly describe all the hyperparameters of all the methods used to make Fig. 3 in Appendix D. **Baselines.** We compare our algorithms with 4 baselines. Diffusion policies [14] use high performing diffusion model architectures. We use both the convolutional and transformer (DiffPolicy-C and DiffPolicy-T) variant of the diffusion policy. VQ-BeT [52] uses VQ-VAEs [83] for discretizing actions and learns a transformer model over chunked representations. BeT [74] is similar to VQ-BeT but uses K-means for action chunking.

Results. In Fig. 3 we see that NF-BC outperforms all baselines on PushT and Kitchen and performs competitively in other two tasks. Of all the baselines, NF-BC is the simplest by more than a factor of 2. For example, DiffPolicy-T uses 3 times more hyperparameters than NF-BC. These results suggest that NF policies do not lack in expressivity, compared to both diffusion and auto-regressive policies despite introducing fewer additional hyper-parameters. In fact, NF-BC can achieve these results using just a fully connected network and fraction of parameters compared to diffusion policies (see rightmost plot in Fig. 3). Unlike BeT [74] and VQ-BeT [52], NF-BC does not use autoregressive models or VQ-VAEs (see Fig. 4 for a comparison of architectures). Reducing the number of hyperparameters is especially important for practitioners because it makes implementation easier and decreases the need for hyperparameter tuning.

6.2 Conditional Imitation Learning

In this section, we use our NF architecture with GCBC (Section 4.1, Eq. (8)) for conditional imitation learning (NF-GCBC).

Tasks. We use a total of 45 tasks from OGBench [66] meant to test diverse capabilities like learning from suboptimal trajectories with high dimensional actions, trajectory stitching and long-horizon reasoning. Performance is measured using the average success rate of reaching a goal in 50 independent trials. **Baselines.** We compare with 6 different baselines. GCBC is the GCBC 4.1 algorithm with a gaussian policy, and FM-GCBC is the GCBC 4.1 algorithm with a flow-matching based policy [56]. The velocity field for FM-GCBC is a fully connected network trained using flow matching. FM-GCBC is the closest baseline to NF-GCBC as it uses the same underlying algorithm, uses a fully connected network like NF-GCBC, and uses an expressive family of policy models. GCIQL [47] is an offline RL algorithm that learns the optimal value function corresponding to the best actions in the dataset. QRL [86] uses a quasimetric architecture to learn the optimal value function and CRL [24] uses contrastive learning to estimate behavior policy’s value function.

Results. In Fig. 5 (left), we see that NF-GCBC exceeds the performance (often significantly) of GCBC on 40/45 tasks. This underscores the importance of using an expressive policy with the GCBC algorithm. In Fig. 5 (right), NF-GCBC, despite being a BC based algorithm, outperforms

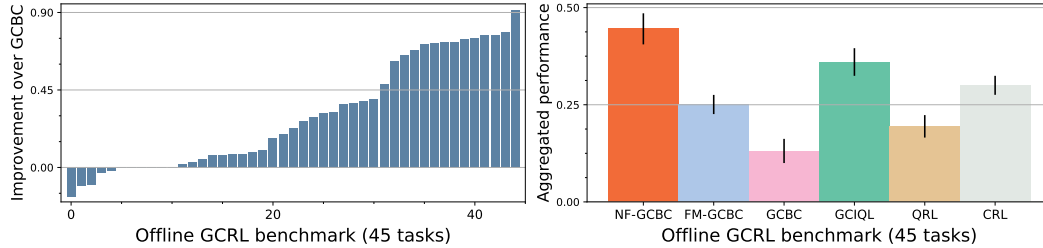


Figure 5: **Conditional Imitation Learning.** (Left) NF-GCBC exceeds its gaussian counterpart GCBC on 40/45 tasks, demonstrates that using expressive models like NFs can significantly improve performance. (Right) Despite being a BC-based algorithm, NF-GCBC outperforms all offline RL baselines across 45 tasks. NF-GCBC performs 77% better than FM-GCBC which is the closest baseline that uses a flow matching policy with GCBC.

all baselines, including dedicated offline RL algorithms. We have added separate task wise plots in Appendix C. NF-GCBC outperforms FM-GCBC, which is the closest baseline, by 77%. While this does not necessarily imply that NFs are more expressive than flow-matching models, we hypothesize that all else being equal (e.g., fully connected architectures and identical underlying algorithms), NFs are better able to imitate the data using simple architectures as they directly optimize for log likelihoods. Flow matching models on the other hand estimate probabilities indirectly (by learning an SDE / ODE), and might require more complex architectures (transformers or convolutional networks) to work well.

6.3 Offline RL

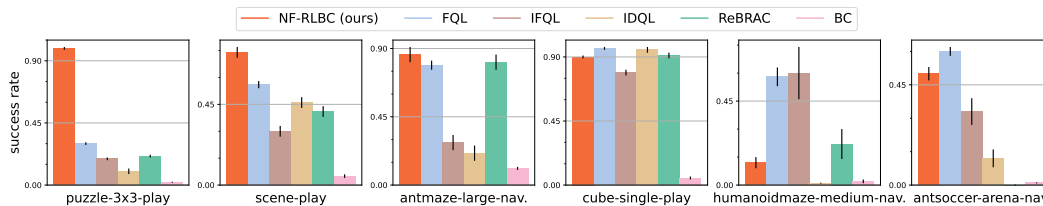


Figure 6: **Offline RL.** NF-RLBC outperforms all baselines on 15/30 tasks, and achieves top 2 results on 10/30 tasks. Notably, NF-RLBC achieves much higher results than all baselines on puzzle-3x3-play and scene-play, which require the most long horizon and sequential reasoning. For example, on puzzle-3x3-play NF-RLBC performs 230% better than the next best baseline.

While NF-GCBC performs better than offline RL algorithms on average, there are certain tasks like puzzle-3x3-play where only TD based methods succeed (Appendix C). This task, and many others as we will see, require learning a value function and accurately extracting behaviors from it. Fortunately, NFs can be trained using both VI and MLE (3). This allows us to train MaxEnt RL+BC (Section 4.2, Eq. (9)) using our NF architecture as a policy (NF-RLBC).

Tasks. We use a total of 30 tasks from prior work [67] testing offline RL with expressive policies. Each task has a goal which requires completing K subtasks. At each step, the agent gets a reward equal to the negative of the number of subtasks left to be completed. For our experiments, we choose tasks that cover a diverse set of challenges and robots. Tasks like humanoidmaze-medium-navigate and antmaze-medium-navigate contain diverse suboptimal trajectories and high dimensional actions. Antsoccer-arena-navigate requires controlling a quadruped agent to dribble a ball to a goal location. Scene-play requires manipulating multiple objects and puzzle-3x3-play requires combinatorial generalization and long-horizon reasoning. We hypothesize that the Q function for the some of these tasks (esp manipulation tasks like puzzle and scene which require long horizon reasoning) can have narrow modes of good actions and a large number of bad actions. Hence using direct gradient based optimization can be crucial to search for good actions. **Baselines.** We choose 5 representative baselines. BC performs BC with a gaussian policy, ReBRAC [82] is an offline RL algorithm with a gaussian policy that achieves impressive results on prior benchmarks [26]. IDQL [36] uses importance resampling to improve over a diffusion policy. IFQL is the flow counterpart of IDQL [67]. FQL [67] is a strong offline RL algorithm that distills a flow-matching policy into a one-step policy, while jointly maximizing the Q-function. Notably, all offline RL algorithms (IDQL,

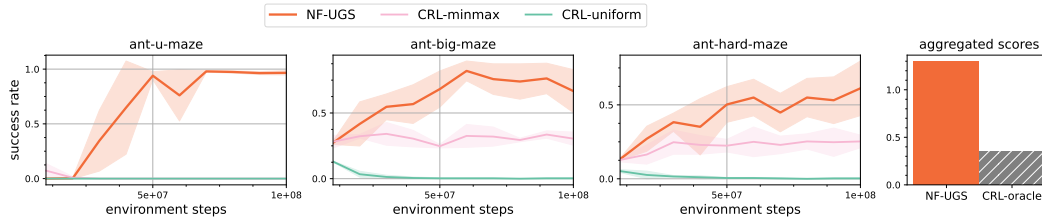


Figure 7: **GCRL**. (first 3 from left) NF-UGS consistently outperforms other unsupervised baselines. (rightmost) NF-UGS achieves higher asymptotic success rates than the CRL-oracle averaged across all tasks. Note that CRL-oracle makes extra assumptions about the availability of test-time goals.

IFQL, FQL) have to incorporate additional components—such as distillation or resampling—to leverage policy expressiveness.

Results. Figure 6, shows that on average NF-RLBC outperforms all baselines on 15/30 tasks, and achieves top 2 results on 10/30 tasks. Notably, NF-RLBC achieves much higher results than all baselines on puzzle-3x3-play and scene-play, which require most long horizon and sequential reasoning (on puzzle-3x3-play NF-RLBC performs 230% better than the next best baseline). NF-RLBC is able to search for good actions because it directly uses gradient based optimization to backpropagate action gradients through the policy. All other offline RL algorithms with expressive policy classes (IDQL, IFQL, FQL) have to use extra intermediate steps.

6.4 Goal Conditioned RL

In this section, we use our NF architecture to estimate both the Q-function (Eq. (11)) and the coverage density (Eq. (12)). Both quantities model the distribution over the same random variable (future goals), with the Q-function conditioned on a state-action pair. We use a single neural network to estimate both by employing a masking scheme to indicate the presence or absence of conditioning [38]. We then train a goal-conditioned policy to maximize the Q-function in a standard actor-critic setup, and sample training goals using the canonical UGS algorithm (Section 4.3), resulting in our NF-UGS method.

Tasks. We use three problems from the UGS literature [68, 9] ant-u-maze, ant-big-maze and ant-hard-maze. These environments are difficult because the goal test distribution is unknown, and success requires thorough exploration of the entire maze. **Baselines.** We compare against three baselines. CRL-oracle [24, 9] uses contrastive learning to estimate the Q-function and serves as an oracle baseline as it uses test goals $p_{\text{test}}(g)$ to collect data during training. CRL-uniform is a variant that samples goals uniformly from the replay buffer, while CRL-minmax selects goals with the lowest Q-value from the initial state of the MDP – intuitively targeting the goals the agent believes are hardest to reach. The aim of these comparisons isn’t to propose a state of the art method, but rather to check whether NFs can efficiently estimate the coverage densities of the non-stationary RL data for unsupervised exploration. **Results.** These experiments aim to evaluate whether NFs can efficiently estimate both the Q-function and the coverage density. As shown in Fig. 7, NF-UGS outperforms all baselines, and notably the oracle algorithm as well (aggregated score is the average of the final success rates across all three tasks). Unlike the minmax strategy, which plateaus over time, NF-UGS continues to improve by sampling goals to maximize the entropy of the coverage distribution [68].

7 Conclusion

In this paper, we view RL problems from a probabilistic perspective, asking: which probabilistic models provide the capabilities necessary for efficient RL? We argue that NFs offer a compelling answer. NFs outperform strong baselines across diverse RL settings, often with fewer parameters and lower compute, leading to simpler algorithms. By making density estimation simpler and effective, we hope our work opens new avenues for areas such as distributional RL, bayesian RL, and RL safety.

A primary limitation of NFs is that they have restrictive architectures, in that they have to be invertible. Nevertheless, there is a rich line of work characterizing which NF architectures are universal [20, 16, 64]. Another limitation of our work is that we do not explore new NF architectures; the design we use is mainly adapted from prior work (Section 5).

Acknowledgments and Disclosure of Funding

The authors are pleased to acknowledge that the work reported on in this paper was substantially performed using the Princeton Research Computing resources at Princeton University which is consortium of groups led by the Princeton Institute for Computational Science and Engineering (PICSciE) and Office of Information Technology’s Research Computing. The authors thank Emmanuel Bengio, Liv d’Aliberti and Eva Yi Xie for their detailed reviews on our initial drafts. The authors thank Seohong Park for providing code for some baselines and Catherine Ji for helping find a bug in our code. The authors also thank the members of Princeton RL lab for helpful discussions.

References

- [1] Agarwal, R., Schuurmans, D., and Norouzi, M. (2020). An optimistic perspective on offline reinforcement learning. In III, H. D. and Singh, A., editors, *Proceedings of the 37th International Conference on Machine Learning*, volume 119 of *Proceedings of Machine Learning Research*, pages 104–114. PMLR.
- [2] Ajay, A., Du, Y., Gupta, A., Tenenbaum, J., Jaakkola, T., and Agrawal, P. (2023). Is conditional generative modeling all you need for decision-making?
- [3] Ba, J. L., Kiros, J. R., and Hinton, G. E. (2016). Layer normalization.
- [4] Bain, M. and Sammut, C. (1995). A framework for behavioural cloning. In *Machine Intelligence 15*.
- [5] Bengio, E., Jain, M., Korablyov, M., Precup, D., and Bengio, Y. (2021). Flow network based generative models for non-iterative diverse candidate generation.
- [6] Bengio, Y., Lahlou, S., Deleu, T., Hu, E. J., Tiwari, M., and Bengio, E. (2023). Gflownet foundations.
- [7] Black, K., Brown, N., Driess, D., Esmail, A., Equi, M., Finn, C., Fusai, N., Groom, L., Hausman, K., Ichter, B., Jakubczak, S., Jones, T., Ke, L., Levine, S., Li-Bell, A., Mothukuri, M., Nair, S., Pertsch, K., Shi, L. X., Tanner, J., Vuong, Q., Walling, A., Wang, H., and Zhilinsky, U. (2024). π_0 : A vision-language-action flow model for general robot control.
- [8] Blei, D. M., Kucukelbir, A., and and, J. D. M. (2017). Variational inference: A review for statisticians. *Journal of the American Statistical Association*, 112(518):859–877.
- [9] Bortkiewicz, M., Pałucki, W., Myers, V., Dziarmaga, T., Arczewski, T., Kuciński, Ł., and Eysenbach, B. (2025). Accelerating goal-conditioned reinforcement learning algorithms and research. In *The Thirteenth International Conference on Learning Representations*.
- [10] Brohan, A., Brown, N., Carbajal, J., Chebotar, Y., Dabis, J., Finn, C., Gopalakrishnan, K., Hausman, K., Herzog, A., Hsu, J., , et al. (2023). Rt-1: Robotics transformer for real-world control at scale.
- [11] Chao, C.-H., Feng, C., Sun, W.-F., Lee, C.-K., See, S., and Lee, C.-Y. (2024). Maximum entropy reinforcement learning via energy-based normalizing flow. In *The Thirty-eighth Annual Conference on Neural Information Processing Systems*.
- [12] Chebotar, Y., Vuong, Q., Hausman, K., Xia, F., Lu, Y., Irpan, A., Kumar, A., Yu, T., Herzog, A., Pertsch, K., Gopalakrishnan, K., Ibarz, J., Nachum, O., Sontakke, S. A., Salazar, G., Tran, H. T., Peralta, J., Tan, C., Manjunath, D., Singh, J., Zitkovich, B., Jackson, T., Rao, K., Finn, C., and Levine, S. (2023). Q-transformer: Scalable offline reinforcement learning via autoregressive q-functions. In Tan, J., Toussaint, M., and Darvish, K., editors, *Proceedings of The 7th Conference on Robot Learning*, volume 229 of *Proceedings of Machine Learning Research*, pages 3909–3928. PMLR.
- [13] Chen, L., Lu, K., Rajeswaran, A., Lee, K., Grover, A., Laskin, M., Abbeel, P., Srinivas, A., and Mordatch, I. (2021). Decision transformer: Reinforcement learning via sequence modeling. In Beygelzimer, A., Dauphin, Y., Liang, P., and Vaughan, J. W., editors, *Advances in Neural Information Processing Systems*.
- [14] Chi, C., Xu, Z., Feng, S., Cousineau, E., Du, Y., Burchfiel, B., Tedrake, R., and Song, S. (2024). Diffusion policy: Visuomotor policy learning via action diffusion.
- [15] Collaboration, E., O’Neill, A., Rehman, A., Gupta, A., Maddukuri, A., Gupta, A., Padalkar, A., Lee, A., Pooley, A., Gupta, A., Mandelkar, A., et al. (2024). Open x-embodiment: Robotic learning datasets and rt-x models.

- [16] Cornish, R., Caterini, A., Deligiannidis, G., and Doucet, A. (2020). Relaxing bijectivity constraints with continuously indexed normalising flows. In III, H. D. and Singh, A., editors, *Proceedings of the 37th International Conference on Machine Learning*, volume 119 of *Proceedings of Machine Learning Research*, pages 2133–2143. PMLR.
- [17] Ding, Y., Florensa, C., Abbeel, P., and Phielipp, M. (2019). Goal-conditioned imitation learning. In Wallach, H., Larochelle, H., Beygelzimer, A., d’Alché-Buc, F., Fox, E., and Garnett, R., editors, *Advances in Neural Information Processing Systems*, volume 32. Curran Associates, Inc.
- [18] Dinh, L., Krueger, D., and Bengio, Y. (2014). Nice: Non-linear independent components estimation. *arXiv: Learning*.
- [19] Dinh, L., Sohl-Dickstein, J., and Bengio, S. (2017). Density estimation using real NVP. In *International Conference on Learning Representations*.
- [20] Draxler, F., Wahl, S., Schnörr, C., and Köthe, U. (2024). On the Universality of Volume-Preserving and Coupling-Based Normalizing Flows. *arXiv preprint arXiv:2402.06578*.
- [21] Emmons, S., Eysenbach, B., Kostrikov, I., and Levine, S. (2022). Rvs: What is essential for offline RL via supervised learning? In *International Conference on Learning Representations*.
- [22] Eysenbach, B., Salakhutdinov, R., and Levine, S. (2021). C-learning: Learning to achieve goals via recursive classification. In *International Conference on Learning Representations*.
- [23] Eysenbach, B., Udatha, S., Salakhutdinov, R. R., and Levine, S. (2022a). Imitating past successes can be very suboptimal. In Koyejo, S., Mohamed, S., Agarwal, A., Belgrave, D., Cho, K., and Oh, A., editors, *Advances in Neural Information Processing Systems*, volume 35, pages 6047–6059. Curran Associates, Inc.
- [24] Eysenbach, B., Zhang, T., Levine, S., and Salakhutdinov, R. (2022b). Contrastive learning as goal-conditioned reinforcement learning. In Oh, A. H., Agarwal, A., Belgrave, D., and Cho, K., editors, *Advances in Neural Information Processing Systems*.
- [25] Florensa, C., Held, D., Geng, X., and Abbeel, P. (2018). Automatic goal generation for reinforcement learning agents. In Dy, J. and Krause, A., editors, *Proceedings of the 35th International Conference on Machine Learning*, volume 80 of *Proceedings of Machine Learning Research*, pages 1515–1528. PMLR.
- [26] Fu, J., Kumar, A., Nachum, O., Tucker, G., and Levine, S. (2021). D4rl: Datasets for deep data-driven reinforcement learning.
- [27] Fujimoto, S. and Gu, S. S. (2021). A minimalist approach to offline reinforcement learning. In Ranzato, M., Beygelzimer, A., Dauphin, Y., Liang, P., and Vaughan, J. W., editors, *Advances in Neural Information Processing Systems*, volume 34, pages 20132–20145. Curran Associates, Inc.
- [28] Fujimoto, S., Meger, D., and Precup, D. (2019). Off-policy deep reinforcement learning without exploration. In Chaudhuri, K. and Salakhutdinov, R., editors, *Proceedings of the 36th International Conference on Machine Learning*, volume 97 of *Proceedings of Machine Learning Research*, pages 2052–2062. PMLR.
- [29] Ghosh, D., Gupta, A., Reddy, A., Fu, J., Devin, C., Eysenbach, B., and Levine, S. (2019). Learning to reach goals via iterated supervised learning. *arXiv preprint arXiv:1912.06088*.
- [30] Graikos, A., Malkin, N., Jovic, N., and Samaras, D. (2022). Diffusion models as plug-and-play priors. In Oh, A. H., Agarwal, A., Belgrave, D., and Cho, K., editors, *Advances in Neural Information Processing Systems*.
- [31] Grigsby, J., Fan, L., and Zhu, Y. (2024). AMAGO: Scalable in-context reinforcement learning for adaptive agents. In *The Twelfth International Conference on Learning Representations*.
- [32] Haarnoja, T., Hartikainen, K., Abbeel, P., and Levine, S. (2018a). Latent space policies for hierarchical reinforcement learning. In Dy, J. and Krause, A., editors, *Proceedings of the 35th International Conference on Machine Learning*, volume 80 of *Proceedings of Machine Learning Research*, pages 1851–1860. PMLR.
- [33] Haarnoja, T., Zhou, A., Abbeel, P., and Levine, S. (2018b). Soft actor-critic: Off-policy maximum entropy deep reinforcement learning with a stochastic actor. In Dy, J. and Krause, A., editors, *Proceedings of the 35th International Conference on Machine Learning*, volume 80 of *Proceedings of Machine Learning Research*, pages 1861–1870. PMLR.
- [34] Hafner, D., Lillicrap, T., Fischer, I., Villegas, R., Ha, D., Lee, H., and Davidson, J. (2019). Learning latent dynamics for planning from pixels. In Chaudhuri, K. and Salakhutdinov, R., editors, *Proceedings of the 36th International Conference on Machine Learning*, volume 97 of *Proceedings of Machine Learning Research*, pages 2555–2565. PMLR.

- [35] Hafner, D., Pasukonis, J., Ba, J., and Lillicrap, T. (2024). Mastering diverse domains through world models.
- [36] Hansen-Estruch, P., Kostrikov, I., Janner, M., Kuba, J. G., and Levine, S. (2023). Idql: Implicit q-learning as an actor-critic method with diffusion policies.
- [37] Ho, J., Jain, A., and Abbeel, P. (2020). Denoising diffusion probabilistic models.
- [38] Ho, J. and Salimans, T. (2022). Classifier-free diffusion guidance.
- [39] Huang, C.-W., Krueger, D., Lacoste, A., and Courville, A. (2018). Neural autoregressive flows. In Dy, J. and Krause, A., editors, *Proceedings of the 35th International Conference on Machine Learning*, volume 80 of *Proceedings of Machine Learning Research*, pages 2078–2087. PMLR.
- [40] Janner, M., Du, Y., Tenenbaum, J., and Levine, S. (2022). Planning with diffusion for flexible behavior synthesis. In Chaudhuri, K., Jegelka, S., Song, L., Szepesvari, C., Niu, G., and Sabato, S., editors, *Proceedings of the 39th International Conference on Machine Learning*, volume 162 of *Proceedings of Machine Learning Research*, pages 9902–9915. PMLR.
- [41] Janner, M., Li, Q., and Levine, S. (2021). Offline reinforcement learning as one big sequence modeling problem. In Ranzato, M., Beygelzimer, A., Dauphin, Y., Liang, P., and Vaughan, J. W., editors, *Advances in Neural Information Processing Systems*, volume 34, pages 1273–1286. Curran Associates, Inc.
- [42] Jordan, M. I. and Bishop, C. M. (2001). An introduction to graphical models. Tutorial material.
- [43] Jordan, M. I., Ghahramani, Z., Jaakkola, T. S., and Saul, L. K. (1999). *An introduction to variational methods for graphical models*, page 105–161. MIT Press, Cambridge, MA, USA.
- [44] Kaelbling, L. P. (1993). Learning to achieve goals. In *International Joint Conference on Artificial Intelligence*.
- [45] Kingma, D. P. and Dhariwal, P. (2018). Glow: Generative flow with invertible 1x1 convolutions. In Bengio, S., Wallach, H., Larochelle, H., Grauman, K., Cesa-Bianchi, N., and Garnett, R., editors, *Advances in Neural Information Processing Systems*, volume 31. Curran Associates, Inc.
- [46] Kingma, D. P., Salimans, T., Jozefowicz, R., Chen, X., Sutskever, I., and Welling, M. (2016). Improved variational inference with inverse autoregressive flow. In Lee, D., Sugiyama, M., Luxburg, U., Guyon, I., and Garnett, R., editors, *Advances in Neural Information Processing Systems*, volume 29. Curran Associates, Inc.
- [47] Kostrikov, I., Nair, A., and Levine, S. (2021). Offline reinforcement learning with implicit q-learning.
- [48] Kumar, A., Fu, J., Soh, M., Tucker, G., and Levine, S. (2019). Stabilizing off-policy q-learning via bootstrapping error reduction. In Wallach, H., Larochelle, H., Beygelzimer, A., d’Alché-Buc, F., Fox, E., and Garnett, R., editors, *Advances in Neural Information Processing Systems*, volume 32. Curran Associates, Inc.
- [49] Kumar, A., Zhou, A., Tucker, G., and Levine, S. (2020). Conservative q-learning for offline reinforcement learning. In Larochelle, H., Ranzato, M., Hadsell, R., Balcan, M., and Lin, H., editors, *Advances in Neural Information Processing Systems*, volume 33, pages 1179–1191. Curran Associates, Inc.
- [50] Laskin, M., Srinivas, A., and Abbeel, P. (2020). CURL: Contrastive unsupervised representations for reinforcement learning. In III, H. D. and Singh, A., editors, *Proceedings of the 37th International Conference on Machine Learning*, volume 119 of *Proceedings of Machine Learning Research*, pages 5639–5650. PMLR.
- [51] Lee, A. X., Nagabandi, A., Abbeel, P., and Levine, S. (2020). Stochastic latent actor-critic: Deep reinforcement learning with a latent variable model. In Larochelle, H., Ranzato, M., Hadsell, R., Balcan, M., and Lin, H., editors, *Advances in Neural Information Processing Systems*, volume 33, pages 741–752. Curran Associates, Inc.
- [52] Lee, S., Wang, Y., Etukuru, H., Kim, H. J., Shafiullah, N. M. M., and Pinto, L. (2024). Behavior generation with latent actions. In Salakhutdinov, R., Kolter, Z., Heller, K., Weller, A., Oliver, N., Scarlett, J., and Berkenkamp, F., editors, *Proceedings of the 41st International Conference on Machine Learning*, volume 235 of *Proceedings of Machine Learning Research*, pages 26991–27008. PMLR.
- [53] Levine, S. (2018). Reinforcement learning and control as probabilistic inference: Tutorial and review.
- [54] Levine, S., Kumar, A., Tucker, G., and Fu, J. (2020). Offline reinforcement learning: Tutorial, review, and perspectives on open problems.
- [55] Lin, F., Hu, Y., Sheng, P., Wen, C., You, J., and Gao, Y. (2025). Data scaling laws in imitation learning for robotic manipulation.

- [56] Lipman, Y., Chen, R. T. Q., Ben-Hamu, H., Nickel, M., and Le, M. (2023). Flow matching for generative modeling.
- [57] Lu, C., Ball, P. J., Teh, Y. W., and Parker-Holder, J. (2023). Synthetic experience replay. In *Thirty-seventh Conference on Neural Information Processing Systems*.
- [58] Ma, Y. J., Sodhani, S., Jayaraman, D., Bastani, O., Kumar, V., and Zhang, A. (2023). VIP: Towards universal visual reward and representation via value-implicit pre-training. In *The Eleventh International Conference on Learning Representations*.
- [59] Micheli, V., Alonso, E., and Fleuret, F. (2023). Transformers are sample-efficient world models. In *The Eleventh International Conference on Learning Representations*.
- [60] Mnih, V., Kavukcuoglu, K., Silver, D., Graves, A., Antonoglou, I., Wierstra, D., and Riedmiller, M. (2013). Playing atari with deep reinforcement learning. *arXiv preprint arXiv:1312.5602*.
- [61] Myers, V., Zheng, C., Dragan, A. D., Levine, S., and Eysenbach, B. (2024). Learning temporal distances: Contrastive successor features can provide a metric structure for decision-making. In *ICML*.
- [62] Ni, T., Eysenbach, B., and Salakhutdinov, R. (2022). Recurrent model-free RL can be a strong baseline for many POMDPs. In Chaudhuri, K., Jegelka, S., Song, L., Szepesvari, C., Niu, G., and Sabato, S., editors, *Proceedings of the 39th International Conference on Machine Learning*, volume 162 of *Proceedings of Machine Learning Research*, pages 16691–16723. PMLR.
- [63] OpenAI, O., Plappert, M., Sampedro, R., Xu, T., Akkaya, I., Kosaraju, V., Welinder, P., D’Sa, R., Petron, A., d. O. Pinto, H. P., Paino, A., Noh, H., Weng, L., Yuan, Q., Chu, C., and Zaremba, W. (2021). Asymmetric self-play for automatic goal discovery in robotic manipulation.
- [64] Papamakarios, G., Nalisnick, E., Rezende, D. J., Mohamed, S., and Lakshminarayanan, B. (2021). Normalizing flows for probabilistic modeling and inference. *Journal of Machine Learning Research*, 22(57):1–64.
- [65] Papamakarios, G., Pavlakou, T., and Murray, I. (2017). Masked autoregressive flow for density estimation. In Guyon, I., Luxburg, U. V., Bengio, S., Wallach, H., Fergus, R., Vishwanathan, S., and Garnett, R., editors, *Advances in Neural Information Processing Systems*, volume 30. Curran Associates, Inc.
- [66] Park, S., Frans, K., Eysenbach, B., and Levine, S. (2025a). OGBench: Benchmarking offline goal-conditioned RL. In *The Thirteenth International Conference on Learning Representations*.
- [67] Park, S., Li, Q., and Levine, S. (2025b). Flow q-learning. *ArXiv*.
- [68] Pitis, S., Chan, H., Zhao, S., Stadie, B., and Ba, J. (2020). Maximum entropy gain exploration for long horizon multi-goal reinforcement learning. In III, H. D. and Singh, A., editors, *Proceedings of the 37th International Conference on Machine Learning*, volume 119 of *Proceedings of Machine Learning Research*, pages 7750–7761. PMLR.
- [69] Pomerleau, D. A. (1988). *Alvinn: An autonomous land vehicle in a neural network*. In Touretzky, D., editor, *Advances in Neural Information Processing Systems*, volume 1. Morgan-Kaufmann.
- [70] Pong, V. H., Dalal, M., Lin, S., Nair, A., Bahl, S., and Levine, S. (2020). Skew-fit: State-covering self-supervised reinforcement learning.
- [71] Ren, A. Z., Lidard, J., Ankile, L. L., Simeonov, A., Agrawal, P., Majumdar, A., Burchfiel, B., Dai, H., and Simchowitz, M. (2024). Diffusion policy optimization.
- [72] Rezende, D. and Mohamed, S. (2015). Variational inference with normalizing flows. In Bach, F. and Blei, D., editors, *Proceedings of the 32nd International Conference on Machine Learning*, volume 37 of *Proceedings of Machine Learning Research*, pages 1530–1538, Lille, France. PMLR.
- [73] Sermanet, P., Lynch, C., Chebotar, Y., Hsu, J., Jang, E., Schaal, S., Levine, S., and Brain, G. (2018). Time-contrastive networks: Self-supervised learning from video. In *2018 IEEE International Conference on Robotics and Automation (ICRA)*, pages 1134–1141.
- [74] Shafiqullah, N. M. M., Cui, Z. J., Altanzaya, A., and Pinto, L. (2022). Behavior transformers: Cloning $\$k\$$ modes with one stone. In Oh, A. H., Agarwal, A., Belgrave, D., and Cho, K., editors, *Advances in Neural Information Processing Systems*.
- [75] Singh, A., Liu, H., Zhou, G., Yu, A., Rhinehart, N., and Levine, S. (2021). Parrot: Data-driven behavioral priors for reinforcement learning. In *International Conference on Learning Representations*.

- [76] Sohl-Dickstein, J., Weiss, E. A., Maheswaranathan, N., and Ganguli, S. (2015). Deep unsupervised learning using nonequilibrium thermodynamics.
- [77] Song, Y., Dhariwal, P., Chen, M., and Sutskever, I. (2023). Consistency models.
- [78] Song, Y., Sohl-Dickstein, J., Kingma, D. P., Kumar, A., Ermon, S., and Poole, B. (2021). Score-based generative modeling through stochastic differential equations.
- [79] Stooke, A., Lee, K., Abbeel, P., and Laskin, M. (2021). Decoupling representation learning from reinforcement learning. In Meila, M. and Zhang, T., editors, *Proceedings of the 38th International Conference on Machine Learning*, volume 139 of *Proceedings of Machine Learning Research*, pages 9870–9879. PMLR.
- [80] Sukhbaatar, S., Lin, Z., Kostrikov, I., Synnaeve, G., Szlam, A., and Fergus, R. (2018). Intrinsic motivation and automatic curricula via asymmetric self-play.
- [81] Tabak, E. and Vanden-Eijnden, E. (2010). Density estimation by dual ascent of the log-likelihood. *Communications in Mathematical Sciences*, 8(1):217–233.
- [82] Tarasov, D., Kurenkov, V., Nikulin, A., and Kolesnikov, S. (2023). Revisiting the minimalist approach to offline reinforcement learning.
- [83] van den Oord, A., Vinyals, O., and Kavukcuoglu, K. (2017). Neural discrete representation learning. In Guyon, I., Luxburg, U. V., Bengio, S., Wallach, H., Fergus, R., Vishwanathan, S., and Garnett, R., editors, *Advances in Neural Information Processing Systems*, volume 30. Curran Associates, Inc.
- [84] Vaswani, A., Shazeer, N., Parmar, N., Uszkoreit, J., Jones, L., Gomez, A. N., Kaiser, L. u., and Polosukhin, I. (2017). Attention is all you need. In Guyon, I., Luxburg, U. V., Bengio, S., Wallach, H., Fergus, R., Vishwanathan, S., and Garnett, R., editors, *Advances in Neural Information Processing Systems*, volume 30. Curran Associates, Inc.
- [85] Venkatraman, S., Khaitan, S., Akella, R. T., Dolan, J., Schneider, J., and Berseth, G. (2024). Reasoning with latent diffusion in offline reinforcement learning. In *The Twelfth International Conference on Learning Representations*.
- [86] Wang, T., Torralba, A., Isola, P., and Zhang, A. (2023). Optimal goal-reaching reinforcement learning via quasimetric learning. In Krause, A., Brunskill, E., Cho, K., Engelhardt, B., Sabato, S., and Scarlett, J., editors, *Proceedings of the 40th International Conference on Machine Learning*, volume 202 of *Proceedings of Machine Learning Research*, pages 36411–36430. PMLR.
- [87] Weng, T., Bajracharya, S. M., Wang, Y., Agrawal, K., and Held, D. (2022). Fabricflownet: Bimanual cloth manipulation with a flow-based policy. In Faust, A., Hsu, D., and Neumann, G., editors, *Proceedings of the 5th Conference on Robot Learning*, volume 164 of *Proceedings of Machine Learning Research*, pages 192–202. PMLR.
- [88] Yarats, D., Zhang, A., Kostrikov, I., Amos, B., Pineau, J., and Fergus, R. (2021). Improving sample efficiency in model-free reinforcement learning from images. *Proceedings of the AAAI Conference on Artificial Intelligence*, 35(12):10674–10681.
- [89] Zhai, S., Zhang, R., Nakkiran, P., Berthelot, D., Gu, J., Zheng, H., Chen, T., Bautista, M. A., Jaitly, N., and Susskind, J. (2024). Normalizing flows are capable generative models. *arXiv preprint arXiv:2412.06329*.
- [90] Zheng, Q., Le, M., Shaul, N., Lipman, Y., Grover, A., and Chen, R. T. (2023). Guided flows for generative modeling and decision making. *arXiv preprint arXiv:2311.13443*.
- [91] Łukasz Kaiser, Babaeizadeh, M., Miłos, P., Osipiński, B., Campbell, R. H., Czechowski, K., Erhan, D., Finn, C., Kozakowski, P., Levine, S., Mohiuddin, A., Sepassi, R., Tucker, G., and Michalewski, H. (2020). Model based reinforcement learning for atari. In *International Conference on Learning Representations*.

A Implementation details.

In this section we provide all the implementation details as well as hyper-parameters used for all the algorithms in our experiments – NF-BC, NF-GCBC, NF-RLBC, and NF-UGS. Unless specified otherwise, we chose common hyper-parameters used in prior work without tuning.

A.1 Imitation Learning: NF-BC

For all imitation learning, we use a policy with 12 NF blocks. The fully connected networks of the coupling network for each NF block consist of two hidden layers with 512 activations each. We use a fully connected network for the state-goal encoder with 4 hidden layers having 512 activations each.

It is common in the NF literature to add some noise to the training inputs before training an NF using MLE [72, 89]. For NF-BC, we add gaussian noise to the actions before training. Hence, NF-BC models the noisy behavior policy instead $\pi^{a+\text{noise}}(a | s)$. To reduce noise from the obtained samples, Zhai et al. [89] propose a denoising trick:

$$z \sim p_0, y := f^{-1}(z), x := y + \sigma^2 \nabla_y \log p_\theta(x)$$

We use this trick in all our NF-BC experiments. Table 2 contains the values of hyperparameters used by NF-BC. All experiments were done on RTX 3090s, A5000s or A6000s and did not require more than 20 hours. Experiment speed is mostly bottlenecked by intermediate evaluation of BC policies because the environments are slow and the number of rollouts per evaluation is 50. For example, the experiments on the multimodal-ant environment took 20 hours, but on pusht they were finished in less than 90 minutes.

Table 2: **NF-BC**: Hyper-parameters and their values.

Hyper-parameter	Description
channels	512
noise std	0.1
blocks	12
encoder num layers	4
rep dims	512

A.2 Conditional Imitation Learning: NF-GCBC

For all conditional imitation learning experiments, we use a policy with 6 NF blocks. The fully connected networks of the coupling network for each NF block consist of two hidden layers with 256 activations each. We use a fully connected network for the state-goal encoder with 4 hidden layers having 512 activations each. The output representation dimensions are 64. We also employ the denoising trick proposed by [89] and mentioned in Appendix A.1. Table 3 contains the values of hyperparameters used by NF-GCBC. All experiments were done on RTX 3090s, A5000s or A6000s and did not require more than 3 hours each.

Table 3: **NF-GCBC**: Hyper-parameters and their values.

Hyper-parameter	Description
channels	512
noise std	0.1
blocks	6
encoder num layers	4
rep dims	512
Future goal sampling discount	Table 4

Table 4: **NF-GCBC**: Environment values for future goal sampling discount values. For all GCBC algorithms, including the GCBC baselines, we tuned this value in the set $\{0.97, 0.99\}$

Environment Name	Future goals sampling discount value γ
puzzle 3×3 play	0.97
scene play	0.97
cube single play	0.97
cube double play	0.99
humanoidmaze medium navigation	0.97
antmaze large navigation	0.99
antsoccer arena navigation	0.97
antmaze medium stitch	0.97
antsoccer arena stitch	0.97

A.3 Offline RL: NF-RLBC

For all offline RL experiments, we use a policy with 6 NF blocks. The fully connected networks of the coupling network for each NF block consist of two hidden layers with 256 activations each. We use a fully connected network for the state-goal encoder with 4 hidden layers having 512 activations each. The output representation dimensions are 64. Table 5 contains the values of main hyperparameters used by NF-RLBC. All experiments were done on RTX 3090s, A5000s or A6000s and did not require more than 3 hours each.

Table 5: **NF-RLBC**: Hyper-parameters and their values.

Hyper-parameter	Description
channels	512
noise std	0.1
actor entropy coefficient (λ in Eq. (9))	0.0
actor BC loss coefficient (α in Eq. (9))	Table 6
blocks	6
encoder num layers	4
rep dims	512

Table 6: **NF-RLBC**: Environment wise actor BC loss coefficient. We use the same hyperparameter tuning procedure as all the baselines [67]. See App E.2. of Park et al. [67]

Environment Name	Actor BC loss coefficient α
puzzle 3×3 play	10.0
scene play	10.0
antmaze large navigation	1.0
cube single play	10.0
humanoidmaze medium navigation	1.0
antsoccer arena navigation	1.0

A.4 Unsupervised RL: NF-UGS

For all unsupervised RL experiments, we use a goal conditioned value function with 6 NF blocks. The fully connected networks of the coupling network for each NF block consist of two hidden layers with 256 activations each. We use a fully connected network for the state-action encoder with 4 hidden layers having 1024 activations each. We train both the conditional $p_\theta(g | s, a)$ and the unconditional $p_\theta(g)$ using the same network. We apply a mask on the conditional variable inputs with probability 0.1. The discount factor we use is 0.99. We add a gaussian noise with standard deviation 0.05. Because we do not sample from the model in NF-UGS, we do not need to employ the denoising trick. Instead, 1024 random goals from the buffer are sampled and the one with the lowest

marginal density $p_\theta(g)$ is selected for data collection. All experiments were done on RTX 3090s, A5000s or A6000s and did not require more than 20 hours each.

B More details about NF block.

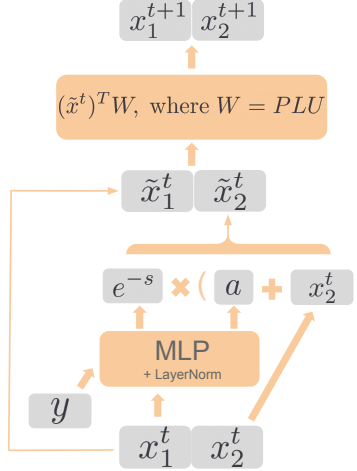


Figure 8: NF block.

It requires the same cost as the coupling of the forward block to calculate the coupling of the inverse block f_θ^{t-1} :

$$\begin{aligned} \tilde{x}_1^t, \tilde{x}_2^t &= \text{split}(\tilde{x}^t), \\ x_1^t &= \tilde{x}_1^t, \\ x_2^t &= \tilde{x}_2^t \times \exp(s_\theta^t(x_1^t, y)) - a_\theta^t(x_1^t, y), \\ x^t &= \text{concat}(x_1^t, x_2^t). \end{aligned}$$

See Fig. 8 for a visualization of each NF block.

C Additional results.

Table 7 and Table 8 contain additional experimental results.

Table 7: Task wise performance for Fig. 5.

Environment	Score
puzzle-3x3-play-v0	0.045±0.005
cube-single-play-v0	0.795±0.109
scene-play-v0	0.420±0.008
cube-double-play-v0	0.351±0.087
antmaze-medium-stitch-v0	0.566±0.068
humanoidmaze-medium-navigate-v0	0.314±0.042
antmaze-large-navigate-v0	0.320±0.055
antsoccer-arena-navigate-v0	0.621±0.007
antsoccer-arena-stitch-v0	0.643±0.016

Table 8: **Task wise performance for Fig. 6.** Scores are mean \pm std.

Environment	Score
antmaze-large-navigate-singletask-task1-v0	0.764 \pm 0.073
antmaze-large-navigate-singletask-task2-v0	0.724 \pm 0.088
antmaze-large-navigate-singletask-task3-v0	0.924 \pm 0.023
antmaze-large-navigate-singletask-task4-v0	0.616 \pm 0.314
antmaze-large-navigate-singletask-task5-v0	0.608 \pm 0.399
antsoccer-arena-navigate-singletask-task1-v0	0.600 \pm 0.122
antsoccer-arena-navigate-singletask-task2-v0	0.556 \pm 0.096
antsoccer-arena-navigate-singletask-task3-v0	0.420 \pm 0.077
antsoccer-arena-navigate-singletask-task4-v0	0.480 \pm 0.061
antsoccer-arena-navigate-singletask-task5-v0	0.336 \pm 0.062
cube-single-play-singletask-task1-v0	0.440 \pm 0.057
cube-single-play-singletask-task2-v0	0.640 \pm 0.087
cube-single-play-singletask-task3-v0	0.768 \pm 0.060
cube-single-play-singletask-task4-v0	0.600 \pm 0.082
cube-single-play-singletask-task5-v0	0.616 \pm 0.067
humanoidmaze-medium-navigate-singletask-task1-v0	0.036 \pm 0.045
humanoidmaze-medium-navigate-singletask-task2-v0	0.188 \pm 0.097
humanoidmaze-medium-navigate-singletask-task3-v0	0.148 \pm 0.072
humanoidmaze-medium-navigate-singletask-task4-v0	0.016 \pm 0.015
humanoidmaze-medium-navigate-singletask-task5-v0	0.208 \pm 0.053
puzzle-3x3-play-singletask-task1-v0	0.996 \pm 0.008
puzzle-3x3-play-singletask-task2-v0	0.996 \pm 0.008
puzzle-3x3-play-singletask-task3-v0	0.976 \pm 0.029
puzzle-3x3-play-singletask-task4-v0	0.996 \pm 0.008
puzzle-3x3-play-singletask-task5-v0	0.996 \pm 0.008
scene-play-singletask-task1-v0	1.000 \pm 0.000
scene-play-singletask-task2-v0	0.880 \pm 0.075
scene-play-singletask-task3-v0	0.988 \pm 0.016
scene-play-singletask-task4-v0	0.856 \pm 0.056
scene-play-singletask-task5-v0	0.000 \pm 0.000

D Hyperparameters used by behavior cloning algorithms based on different probabilistic models.

Table 9: **Hyper-parameters used by NF-BC.**

Hyper-parameter	Description
channels	width of each layer of the coupling MLP network.
noise std	added noise to labels for training the NF using MLE.
blocks	number of NF blocks.
encoder num layers	number of layers in the observation encoder MLP network.
rep dims	output dimension of observation encoder MLP network.

Table 10: Hyper-parameters used by BET.

Hyper-parameter	Description
embedding dims	dimension length for attention vectors.
num layers	number of attention blocks.
num heads	number of heads in attention.
act scale	action scaling parameter.
num bins	number of centroids for k-means.
offset prediction	whether to predict offsets for actions or not.
offset loss scale	action offset prediction loss coefficient.
gamma	focal loss parameter.

Table 11: Hyper-parameters used by DiffPolicy-C.

Hyper-parameter	Description
time-step embedding dims	embedding dimension of diffusion timestep.
down dims	downsampling dimensions for Unet architecture.
kernel size	kernel size for CNNs in Unet.
n groups	number of groups for group normalization.
scheduler train timesteps	Length of the forward diffusion chain while training.
num inference steps	Length of the denoising steps while sampling.
beta schedule type	type of scheduler for noising.
beta start	first-step noise for diffusion scheduler.
beta end	last-step noise for diffusion scheduler.
ema inverse gamma	parameter for ema rate schedule.
ema power	parameter for ema rate schedule.
ema min	minimum value of ema decay rate.
ema max	maximum value of ema decay rate.

Table 12: Hyper-parameters used by DiffPolicy-T.

Hyper-parameter	Description
time-step embedding dims	embedding dimension of diffusion timestep.
embedding dims	dimension length for attention vectors.
num layers	number of attention blocks.
num heads	number of heads in attention.
scheduler train timesteps	Length of the forward diffusion chain while training.
num inference steps	Length of the denoising steps while sampling.
beta schedule type	type of scheduler for noising.
beta start	first-step noise for diffusion scheduler.
beta end	last-step noise for diffusion scheduler.
ema inverse gamma	parameter for ema rate schedule.
ema power	parameter for ema rate schedule.
ema min	minimum value of ema decay rate.
ema max	maximum value of ema decay rate.

Table 13: **Hyper-parameters used by VQ-BET.**

Hyper-parameter	Description
embedding dims	dimension length for attention vectors.
num layers	number of attention blocks.
num heads	number of heads in attention.
action seq len	sequence length used to train the behavior transformer.
vqvae num embed	cookbook size of vqvae.
vqvae embedding dims	embedding dimensions of vqvae codes.
vqvae groups	number of groups in residual vqvae.
encoder loss multiplier	encoder loss coefficient.
offset loss multiplier	action offset prediction loss coefficient.
secondary code multiplier	secondary code prediction loss coefficient.
gamma	focal loss parameter.